ACS Catalysis

Article

Tuning the Selectivity of Palladium Catalysts for Hydroformylation and Semi-Hydrogenation of Alkynes: Experimental and Mechanistic Studies

Jiawang Liu, Zhihong Wei, Ji Yang, Yao Ge, Duo Wei, Ralf Jackstell, Haijun Jiao, and Matthias Beller

ACS Catal., **Just Accepted Manuscript** • DOI: 10.1021/acscatal.0c03614 • Publication Date (Web): 22 Sep 2020

Tuning the Selectivity of Palladium Catalysts for Hydroformylation and Semi-Hydrogenation of Alkynes: Experimental and Mechanistic Studies

Jiawang Liu,[†,∥] Zhihong Wei,[†,‡,∥] Ji Yang,[†,∥] Yao Ge,[†] Duo Wei,[†] Ralf Jackstell,[†] Haijun Jiao,[†,*] Matthias Beller[†,*]

[†] Leibniz-Institut für Katalyse e.V., Albert-Einstein-Str. 29a, Rostock, 18059, Germany

[‡] Institute of Molecular Science, Key Laboratory of Materials for Energy Conversion and Storage of Shanxi Province, Shanxi University , Taiyuan 030006, P. R. China

KEYWORDS : hydroformylation• semi-hydrogenation• alkynes • syngas• mechanism• selectivity

ABSTRACT: Here, we describe a selective palladium catalyst system for chemodivergent functionalization of alkynes with syngas. In the presence of the advanced ligand **L2** bearing 2-pyridyl substituent as a built-in base, either hydroformylation or semi-hydrogenation of diverse alkynes occurs with high chemo- and stereoselectivity under comparable conditions. Mechanistic studies including DFT calculations, kinetic analysis and control experiments revealed that the strength and concentration of the acidic co-catalysts play a decisive role in controlling the chemoselectivity. DFT studies disclosed that the ligand **L2** not only promotes a heterolytic activation of hydrogen similar to FLP (frustrated Lewis pair) systems in the hydrogenolysis step for hydroformylation, but also suppresses CO coordination to promote semi-hydrogenation under strong acid condition. This switchable selectivity provides a strategy in designing catalysts for desired products.

INTRODUCTION

Precise control of selectivity in chemical transformations is amongst the most important subjects in organic chemistry, since this is crucial for the economic and green synthesis of any desired products. Nevertheless, achieving high chemo-, regio-, and/or stereoselectivity even for simple substrates continues to be difficult.[1] While for stoichiometric organic synthesis only limited possibilities exist to regulate selectivity issues, e.g. temperature and solvents, catalytic reactions offer many more possibilities by varying metals, ligands, acids, bases, and additives. Advantageously, for substrates with several reactive centers, applying different catalysts allows one to access different products from the same substrate. This concept is efficiently used in diversity-oriented synthesis for a variety of applications.[2] Notably, in the vast majority of these reactions diverse catalyst systems under completely different conditions are used.[3] In contrast, here we describe a single molecularly-defined catalyst, which allows for either hydrogenation or hydroformylation of alkynes with extremely high selectivity under nearly identical conditions.

Transition metal catalyzed hydroformylation is recognized as the most powerful tool to produce aldehydes in industry.[4] Compared to the well-studied reaction of olefins with syngas,[5][6] the corresponding reaction of alkynes has proven to be many more difficult, although it permits for an atom-economic access of α,β-unsaturated aldehydes.[7][8] The main problem of this latter transformation is the concomitant generation of alkanes and/or alkenes due to side hydrogenation reactions (Scheme 1a). Thus, only few Rh-based catalysts were successfully developed by the groups of Buchwald,[7b] Alper,[7c-d] Breit,[7e] Zhang,[7f] You,[7g] and Girard[7h]. In addition, Pd/phosphine catalysts were introduced for this process by Hidai[8a] and Tao[8b] and co-workers as well as our group[8c].

Scheme 1. Transition metal catalyzed semi-hydrogenation and hydroformylation of alkynes

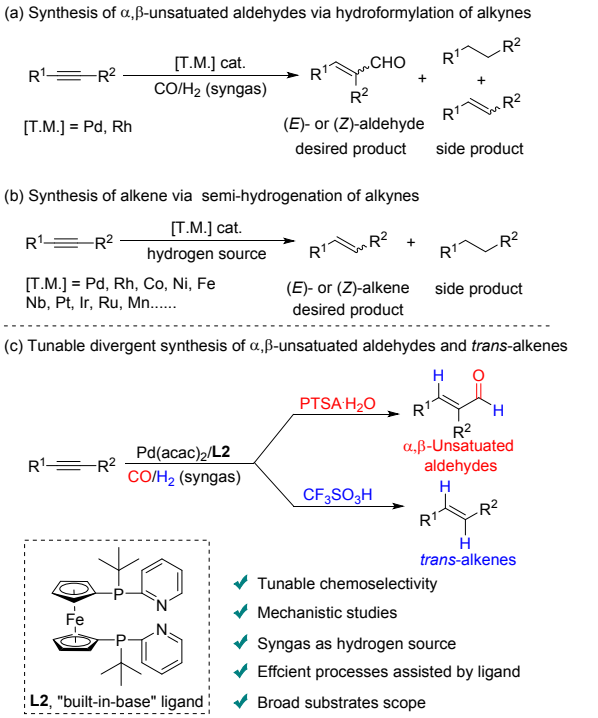

Despite all this progress, a detailed understanding of the factors influencing different reaction pathways is missing so far. Notably, these (unwanted) hydrogenation processes also offer interesting possibilities, as the semi-hydrogenation of alkynes represents an important transformation for the synthesis of various olefins.[9]

Since the original report of Lindlar[10], both hetero- and homogeneous catalysts based on noble[11] and earth-abundant base[12] metals have been developed for the stereoselective synthesis of *Z*- and/or *E*-alkenes in the presence of various hydrogen sources such as hydrogen gas, formic acid, stoichiometric amounts of reductants in water, alcohols and ammonia borane (Scheme 1b). Compared to pure hydrogen gas, syngas (CO/H_2 = 1/1) is scarcely used for reduction reactions, except for its application in the sequential hydroformylation-hydrogenation[13] processes as well as aldehyde reduction[14].

So far, the industrial production of pure hydrogen gas mainly relies on fossil resources leading initially to mixtures of CO and H_2, which are purified afterwards. Therefore, the development of a selective semi-hydrogenation of alkynes with direct utilization of syngas would be interesting, but also challenging. In fact, only few examples were reported using Nb[15], supported Pd,[16] and Rh[17] as catalysts. However, in all these cases the main products are *Z*-alkenes. Complementary to all these works, we disclose highly tunable Pd catalysts, which permit the synthesis of *E*-alkenes (Scheme 1c).

Recently, we introduced a series of bidentate phosphine ligands by incorporating 2-pyridyl substitutents as a built-in base on the phosphorus atoms.[18] Applying some of them in Pd-catalyzed alkoxycarbonylation of alkenes,[18a] dienes[18d] and alkynes[18c], significant improvement of reactivity was achieved. Mechanistic studies revealed the role of the basic nitrogen atom on the 2-pyridyl group as proton shuttle, which accelerates the alcoholysis of the Pd-acyl intermediate and increases the rate of overall reaction.[19] We envisioned that these ligands might also improve the reactivity in Pd-catalyzed hydroformylation of alkynes affording α,β-unsaturated aldehydes in a similar manner.

RESULTS AND DISCUSSION

Condition optimization: Initial studies began with the examination of selected phosphine ligands with built-in base **L1-L4** using diphenylacetylene (**1**) as model substrate to produce α,β-unsaturated aldehyde (**2**). Inspired by previous Pd-catalyzed alkoxycarbonylations 1.0 mol% $Pd(acac)_2$, 4.0 mol% ligand, 16.0 mol% *p*-toluenesulfonic acid monohydrate ($PTSA{\cdot}H_2O$) were used under 50 bar syngas (CO/H_2 = 1/1)]. As shown in Table 1, in the presence of 1,2-bis((*tert*-butyl(pyridin-2-yl)phosphanyl)meth-yl)benzene **L1** as ligand, **2** was obtained in 81% yield with 92/8 stereoselectivity. However, around 10% of a stilbene mixture (**3**) was observed. The yield of **2** was increased to 92% (*E*/*Z* = 94/6), while that of **3** was surpassed to less than 5% by using 1,1'-ferrocenediyl-bis(*tert*-butyl(pyridin-2-yl)phosphine) **L2** as ligand. In the presence of 1,4-bis(*tert*-butyl(pyridin-2-yl)phosphanyl)butane **L3** or 2,2'-bis(*tert*-butyl(pyridin-2-yl)phosphaneyl)-1,1'-binaphtha-lene **L4** (Neolephos), more **3** as side-product was generated without the improvement in stereoselectivity.

For comparison, **L5-L8**, which do not have the built-in base but have the same ligand backbone to **L1-L4**, were also tested. Interestingly, in all cases the **2**/**3** ratio decreased, demonstrating the superiority of **L1-L4** in controlling the chemoselectivity towards **2**. The best result for achieving **2** in high activity and selectivity was found for using **L2**. Thus, this ligand was used in further studies.

Table 1. Pd-catalyzed hydroformylation of diphenylacetylene: Variation of ligands and acids [a]

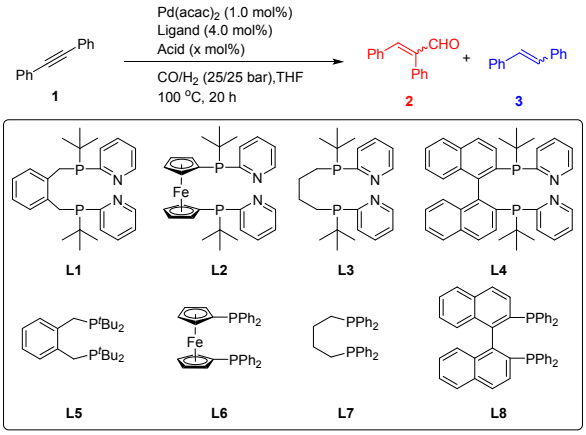

Entry	Ligand	Acid (x)	**2**/**3**[b]	Yield of **2** (%) (*E*/*Z*)[b]
1	**L1**	PTSA (16)	87/13	81 (92/8)
2	**L2**	PTSA (16)	94/6	92 (94/6)
3	**L3**	PTSA (16)	80/20	76 (94/6)
4	**L4**	PTSA (16)	83/17	67 (95/5)
5	**L5**	PTSA (16)	75/25	21 (99/1)
6	**L6**	PTSA (16)	70/30	58 (96/4)
7	**L7**	PTSA (16)	55/45	45 (93/7)
8	**L8**	PTSA (16)	71/29	57 (95/5)
9	**L2**	TFA (16)	89/11	75 (93/7)
10	**L2**	$MeSO_3H$ (16)	94/6	92 (94/6)
11	**L2**	**PTSA (8)**	**95/5**	**94 (97/3)**[c]
12	**L2**	PTSA (32)	82/18	79 (95/5)
13	**L2**	**CF_3SO_3H (16)**	**<1/>99**	**98 (>99/1)**[d]

[a] Unless otherwise noted, all reactions were performed in THF (1.0 mL) at 100 ˚C for 20 h in the presence of diphenylacetylene (**1**, 0.3 mmol), $Pd(acac)_2$ (0.91 mg, 0.003 mmol), acid (x mol%), ligand (0.012 mmol) and CO/H_2 (25/25 bar). [b] The ratio of **2**/**3**, the *E*/*Z* selectivity and the yield were determined by GC analysis using isooctane as the internal standard. [c] The isolated yield of aldehyde **2** was 90%. [d] The isolated yield of alkene (*E*)-**3** was 97%.

Apart from investigating the effect of solvents, temperature, palladium precursors, the impact of the acidic co-catalyst was tested with **L2**. As expected, there was no conversion of substrate without acid. Using trifluoroacetate acid afforded **2** in 75% yield with 89/11 chemoselectivity. Lowering the loading of PTSA to 8.0 mol% gave slight improvement of both chemo- and stereoselectivity (**2**/**3**: 95/5, 94% yield, 97/3 *E*/*Z*). Surprisingly, when triflic acid (HOTf) was used instead of PTSA under otherwise identical reaction conditions, the chemoselectivity switched drastically and **3** is obtained with high yield (98%) and selectivity (*E*/*Z*, >99/1). Notably, no over reduction to the corresponding alkane was detected.

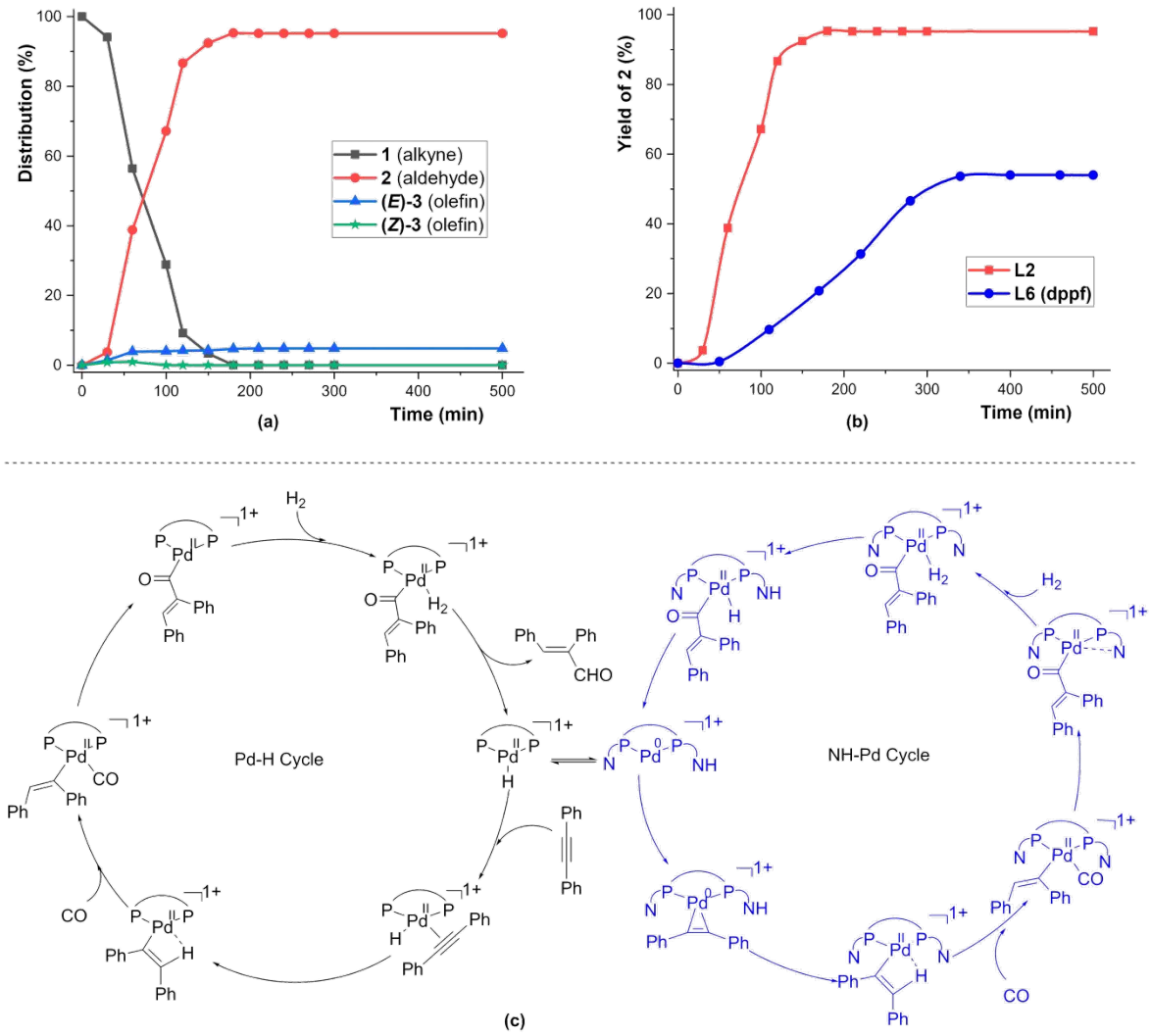

Figure 1. Kinetic studies of Pd-catalyzed hydroformylation of **1** and two proposed possible mechanism: (a) Distribution of compounds for Pd-catalyzed hydroformylation in the presence of **L2**; (b) Comparison of aldehyde yield using **L2** (red) and **L6** (blue) as ligand; (c) Proposed Pd hydride (Pd-H Cycle) and bifunctional (NH-Pd Cycle) mechanism.

Mechanistic studies: To shed more light on this interesting chemoselectivity, mechanistic studies including kinetic analysis, control experiments and DFT calculations were performed. First, the hydroformylation of **1** was investigated under standard conditions. As shown in Figure 1a, (*E*)-**2** is generated from the very beginning along with the gradual consumption of **1** and the distribution of (*E*)-**2** was 94% with 5% of (*E*)-**3** after 3 hours. These results demonstrated clearly that the hydroformylation of **1** was faster than we presented in Table 1 (20 hours). For **L6**, lower activity and selectivity were found (Figure 1b).

To understand the experimentally observed differences in activity and selectivity of **L2** and **L6**, density functional theory computations were carried out (see *Supporting Information* for more details). Here, we used the M06L-SCRF/def2-TZVP[20] computed Gibbs free energies (ΔG, at 373 K) under the consideration of solvation effect (THF) on the basis of the B3PW91-SCRF/TZVP[21] optimized geometries in THF solution for discussion. In all our calculations, we used the real-size systems without constrains and simplifications for both ligands, **L2** and **L6**, as well as their corresponding Pd complexes, **[L2Pd^{II}-H]**$^+$ and **[L6Pd^{II}-H]**$^+$. The analysis into the detailed Gibbs free energy profiles and the critical transition state structures with selected bond parameters are given in *Supporting Information*. For the complexes of **L2**, we used the same diastereomer as rationalized in our previous work.[19a]

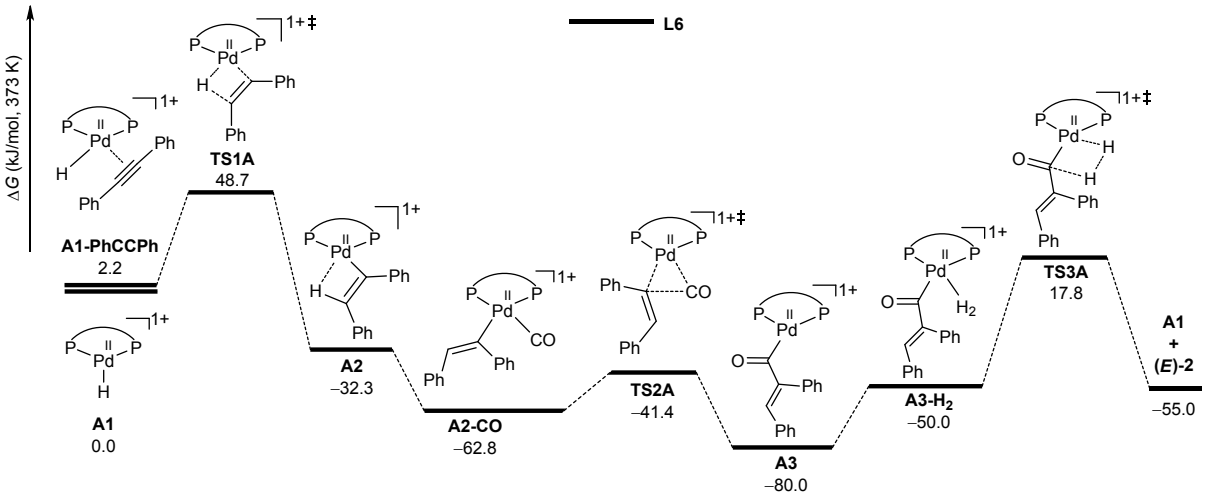

Figure 2. Gibbs free energy (Δ*G*, 373 K) profile for **[L6Pd^{II}-H]**$^{+}$ catalyzed hydroformylation of **1**

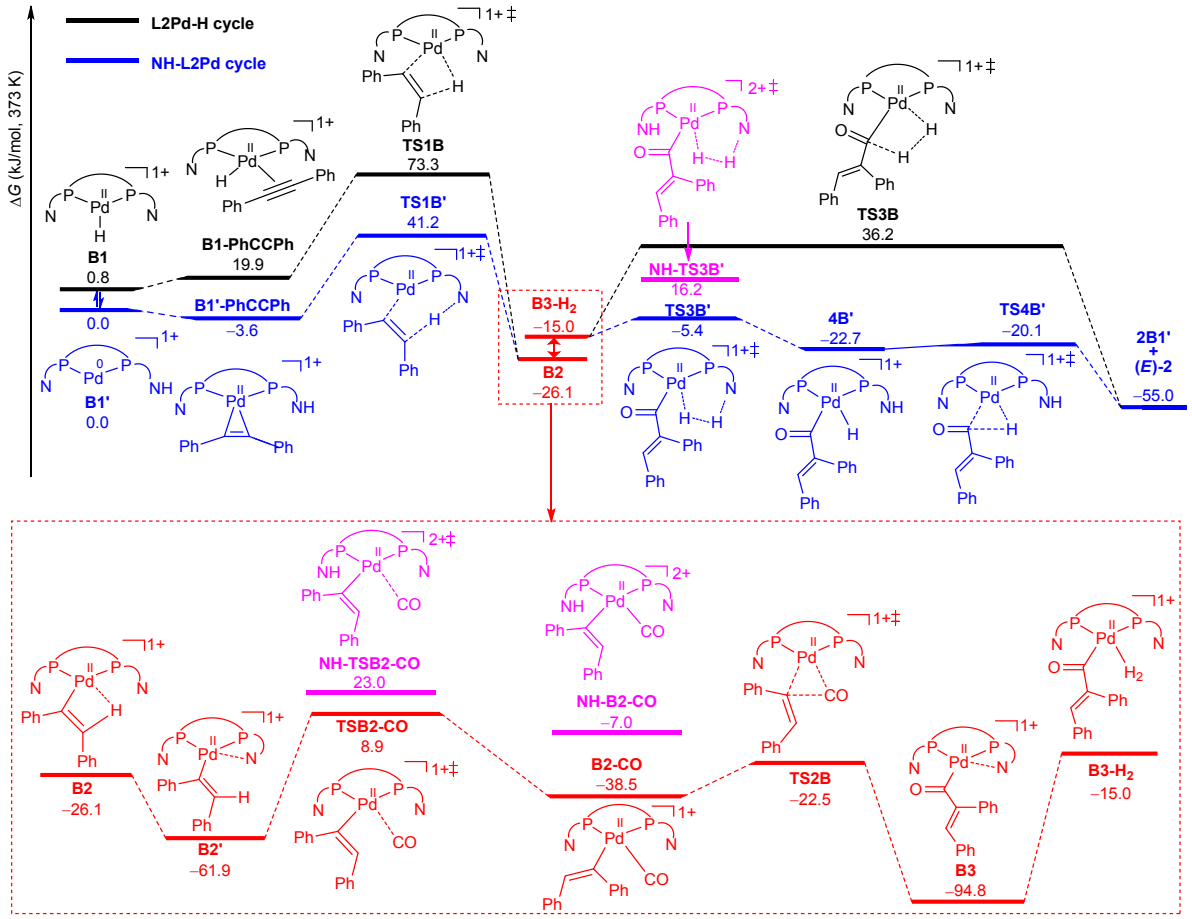

Figure 3. Gibbs free energy (Δ*G*, 373 K) profile of **[L2Pd^{II}-H]**$^{+}$ and **[NH-L2Pd^{0}]**$^{+}$ catalyzed hydroformylation of **1** (**NH-TS3B'** and **NH-TSB2-CO**, in pink, represents the transition states of hydrogenolysis and CO coordination under protonation)

Figure 1c shows the two proposed mechanisms, the well accepted Pd-H cycle [19a, 22] (left side) and the bifunctional NH-Pd cycle [19a, 19c] (right side), in which the built-in 2-pyridyl moiety can facilitate the nucleophilic attack on the Pd-acyl intermediate. Starting from the cationic **[LPd^{II}-H]**$^{+}$ complex, the first step is alkyne coordination and Pd-H insertion with the formation of the alkenyl complex **[LPd^{II}(C(Ph)=CHPh)]**$^{+}$; and the second step is CO coordination and insertion with the formation of the corresponding acyl complex **[LPd^{II}(-CO-C(Ph)=CHPh)]**$^{+}$. The last step is hydrogenolysis of the acyl complex resulting in the formation of 2,3-

diphenylacrylaldehyde (**2**) and the regeneration of the active **[LPd^{II}-H]**$^+$ catalyst.

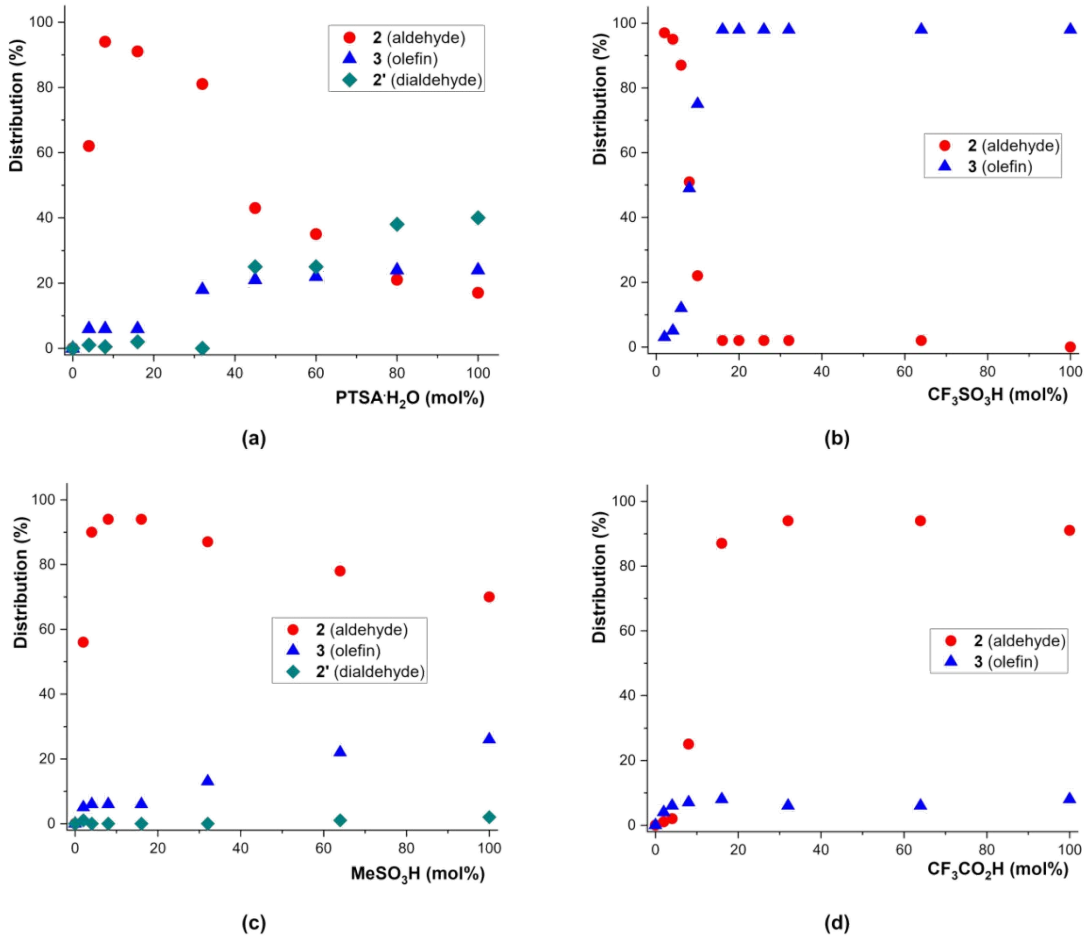

Figure 4. Pd-catalyzed hydroformylation *vs* semi-hydrogenation of **1** under syngas conditions: Influence of acid concentration on the product distribution. Reaction conditions: all reactions were performed in THF (1.0 mL) at 100 ˚C for 20 h in the presence of **1** (0.3 mmol), Pd(acac)$_2$ (0.91 mg, 1.0 mol%) and **L2** (6.1 mg, 4.0 mol%) under CO/H_2 (25/25 bar) atmosphere with specified acid. The distribution of **2** (aldehyde), **3** (olefin) and **2'** (dialdehyde) were determined by GC and GC-MS analysis. (a) The distribution of products using varied amount of PTSA·H_2O; (b) The distribution of products using varied amount of CF_3SO_3H; (c) The distribution of products using varied amount of $MeSO_3H$; (d) The distribution of products using varied amount of CF_3CO_2H.

For **L6** as ligand, the computed Gibbs free energy profile is given in **Figure 2**. It shows that the Pd-H insertion via **TS1A** represents the highest point on Gibbs free energy profiles and has a barrier of 48.7 kJ/mol; the acyl complex (**A3**) represents the resting state and the hydrogenolysis via **TS3A** has an energy span of 98.6 kJ/mol, which is also the effective barrier, and the total reaction is exergonic by 55 kJ/mol.

For **L2** as ligand, both catalytic cycles, Pd-H (black line) and NH-Pd (blue line), are computed (Figure 3). It shows that both cycles differ in two points; the first one is the formation of alkenyl complex via either Pd-H insertion or N-H proton shuttle transfer. It is found that the N-H proton shuttle transfer is more energetically favored than the Pd-H insertion pathway, not only in alkyne coordination (23.5 kJ/mol) but also in the transition state (32.1 kJ/mol). The barrier of NH-Pd cycle is lower than that of the Pd-H cycle by 32.1 kJ/mol, demonstrating the role of the built-in base in lowering the barrier and accelerating the overall reaction. The second point is the product formation either via the direct one step hydrogenolysis of acyl complex through Pd coordination (Pd-H_2, **TS3B**) or by 2-pyridyl-assisted heterolytic dissociation of H_2 forming N-H and Pd-H (**TS3B'** and **B4'**), followed by the Pd-H insertion (**TS4B'**). It shows again that the built-in base assisted pathway is lower in energy than the Pd-H_2 pathway by 41.6 kJ/mol. In both pathways, the transition state of alkenyl complex formation (**TS1B** and **TS1B'**) represents the highest point on the potential energy surface, and the acyl complex (**B3**) is the resting state, and the corresponding effect barrier of rate-determining step of hydrogenolysis is 131.0 and 89.4 kJ/mol, respectively. This demonstrates once more the barrier-lowering role of the built-in base (41.6 kJ/mol). Comparing the more favored pathways using **L2** and **L6** shows that the reaction in the presence of **L2** has lower apparent barrier (41.2 vs. 48.7 kJ/mol) and lower effective barrier (89.4 vs. 98.6 kJ/mol) than that with **L6**. Such differences in barriers agree with the observed activity in Figure 1b, which shows that reaction with **L2** is more active than with **L6**.

It is interesting to note that the transition state (**TS3B'**) for H_2 activation can be regarded as a type of Frustrated Lewis Pair like (FLP) as proposed by Stephan,[23] where the Pd(II) center acts as Lewis acid and the built-in nitrogen atom of the hemilabile 2-pridyl group as Lewis base. In **TS3B'**, the

breaking H–H distance is 0.90 Å and formation N–H distance is 1.57 Å as well as that of Pd–H is 1.72 Å. Apart from the role in lowering the barriers, the built-in base in **L2** also stabilizes the intermediates, i.e., **B2** and **B3**, as compared with the corresponding intermediates (**A2** and **A3**) by using **L6**.

Since the chemoselectivity can be completely switched from **2** to **3** by varying the acid co-catalyst (Table 1), we performed the model reaction in the presence of different acids and studied the effect of acid loading on the product distribution (Figure 4). All these reactions were conducted under similar conditions except the amount of acid. At lower concentration of PTSA·H_2O (<5.0 mol%), the main product was the aldehyde **2** and only very small amounts of olefin **3** were observed (Figure 4a). Slightly increasing the acid concentration to 8 mol%, the yield of **2** reached its maximum along with an increase of **3** and (**2'**) via double hydroformylation (Figure 4a). With a further increase of acid concentration (>40 mol%), the yield of **2** drops drastically, while at the same time, the yields of **3** and dialdehyde (**2'**) increased strongly. At very high acid concentration the formation of the respective acid via hydro-carboxylation due to the presence of H_2O as hydrate in acid can be observed, too. Importantly, for the reaction of (*E*)- or (*Z*)-stilbene in the presence of 1 eq. of PTSA there was no hydroformylation product detectable (*Scheme S2*).

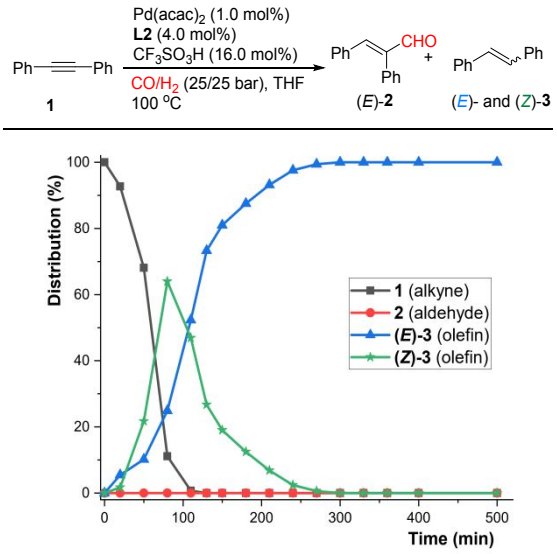

Figure 5. Reaction profile of Pd-catalyzed semihydrogenation of **1**

An even more pronounced chemoselectivity change was observed when using triflic acid (Figure 4b). In fact, in the presence of 2-6 mol% of acid loading, **2** is obtained in high yield as the main product. With increasing CF_3SO_3H concentration, the yield of **2** drops drastically. In contrast, the yield of **3** is negligible at low acid concentration; however, rose rapidly with increasing amount of acid and reached a maximum at about 16 mol% acid. Similar selectivity effects were found for methanesulfonic acid (CH_3SO_3H, Figure 4c) and trifluoroacetic acid (CF_3CO_2H, Figure 4d). Comparing all four acids reveals that PTSA and $MeSO_3H$ have the same distribution patterns, which differ strongly from those of CF_3SO_3H and CF_3CO_2H. In general, the observed chemoselectivity differences can be explained by the strength and concentration of the used acid. For example, triflic acid as the strongest acid (most negative p_{Ka} value –5.21) has the highest chemoselectivity towards the alkene (**3**), while CF_3COOH has the lowest p_{Ka} value (0.23) and led mainly to the aldehyde (**2**) even at high acid concentration.[24] The computed proton affinity of the conjugated bases have the same order (see Supporting Information).

To get more information about the observed changes in chemoselectivity, a reaction profile of the model reaction was performed using triflic acid under the standard conditions. As shown in Figure 5, with increasing reaction time both (*Z*)-**3** and (*E*)-**3** are formed. The concentration of (*Z*)-**3** increased fast to maximum at about 80 minutes and then decreased quickly and vanished at about 270 minutes. In contrast, the concentration of (*E*)-**3** increased steadily and at about 270 minutes it is nearly the single product obtained. This clearly indicates a semi-hydrogenation reaction accompanied with a slower isomerization process from (*Z*)-**3** to (*E*)-**3**. Additional control experiment under the same conditions using (*Z*)-**3** and (*E*)-**3** as starting substrates showed indeed that (*Z*)-**3** is completely isomerized to (*E*)-**3**, while (*E*)-**3** did not react at all (*Scheme S3*). In the whole reaction period (up to 500 minutes), neither hydroformylation products (aldehydes) nor over hydrogenation product (alkane) were observed.

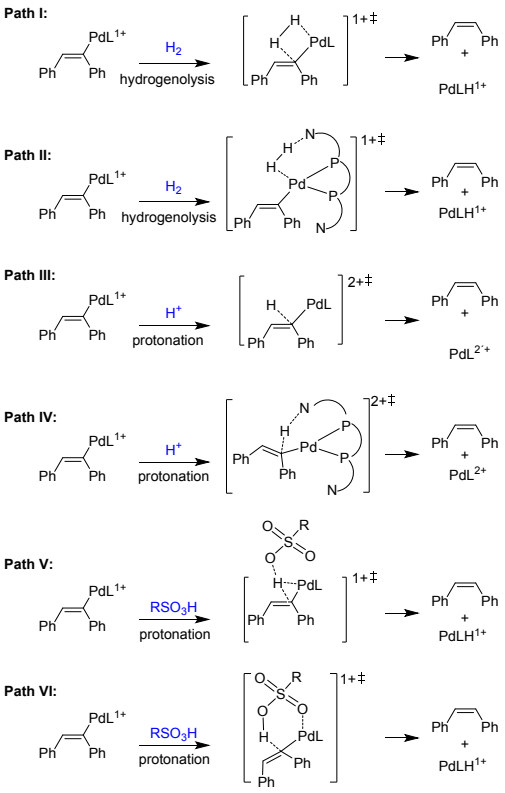

Scheme 2. Proposed mechanism for generation of alkene from Pd-alkenyl complex

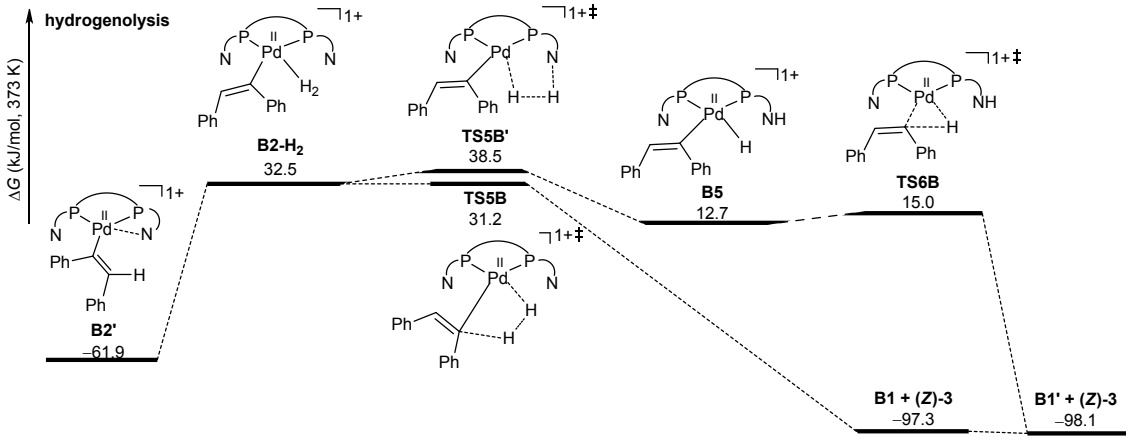

Figure 6. Gibbs free energy profile of **[NH-L2Pd⁰]**⁺ catalyzed semi-hydrogenation of **1** without excess acid.

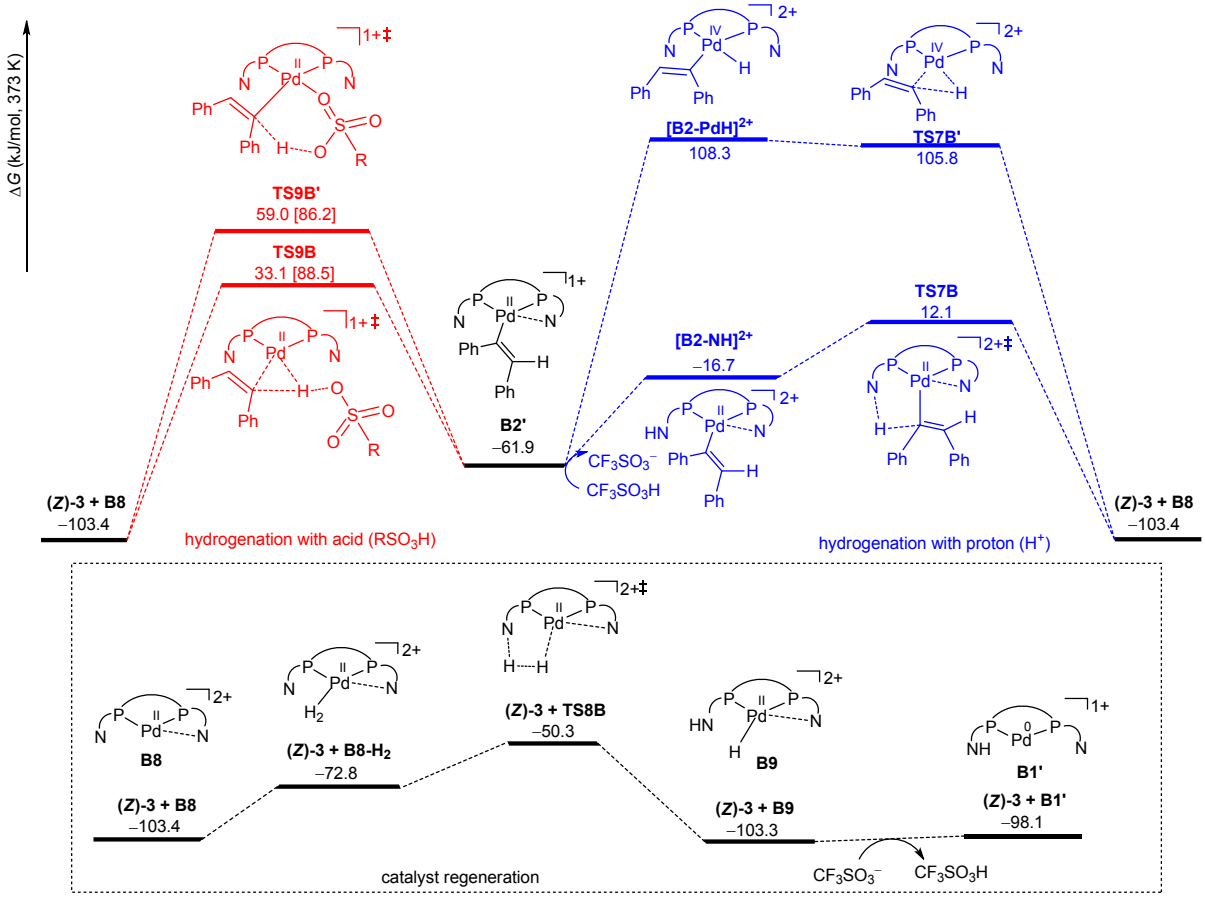

Figure 7. Gibbs free energy profile of **[NH-L2Pd⁰]**⁺ catalyzed semi-hydrogenation of **1** by using CF_3SO_3H and PTSA (red part in square brackets) as co-catalyst

According to the proposed reaction mechanism in Figure 1, the first step of the semi-hydrogenation and hydroformylation reaction is the same. In this respect, the Pd-alkenyl complex (**B2'**, Figure 3) is the key intermediate for either hydrogenolysis or follow up carbonylation reaction. Starting from the alkenyl intermediate (**B2'**), both hydrogenolysis (paths **I** and **II**) and protonation (paths **III-IV**) are proposed (Scheme 2). Since the chemoselectivity is drastically influenced by the acid co-catalyst, we computed the hydrogenolysis step without excess acid and with excess acid to rationalize the observed effects. On the basis of alkenyl complex (**B2'**) without excess acid, both the direct one step hydrogenolysis (path **I**) and the ligand-promoted stepwise H_2 activation and hydride transfer process (path **II**) are computed (Figure 6). It is found that path **I** via **TS5B** has lower apparent barrier than path **II** via **TS5B'** (31.2 vs. 38.5 kJ/mol).

Comparing the Gibbs free energy profiles in Figures 3 and 6 shows that the ligand-promoted H_2 activation and aldehyde (**2**) formation is lower in energy than the direct hydrogenolysis for the formation of (*Z*)-**3** (–5.4 vs. 31.2 kJ/mol); and the formation

of **2** is more preferred kinetically than that of (*Z*)-**3**. Considering the fact that the transition state of CO coordination (**TSB2-CO**, 8.9 kJ/mol) is higher in energy than the ligand-promoted H_2 activation (**TS3B'**, –5.4 kJ/mol) (**Figure 3**), the energy difference to discriminate the chemoselective formation of **2** over **3** is 22.3 kJ/mol (8.9 vs. 31.2 kJ/mol); and this will give an exclusive formation of **2** (>99%) over **3** (<1%). Although slightly overestimated on the basis of the experimentally detected chemoselectivity (Table 1 and Figure 1a, 94%/6%), the computed result is reasonable. Under the conditions with excess acid, the reaction pathways either via direct protonation to the Pd center followed by reductive elimination (path **III**) or via the 2-pyridyl-assisted protonation and reductive elimination (path **IV**) was computed (Figure 7, blue lines). It is found that path **IV** is much favored compared to path **III** in the protonation step (–16.7/[**B2-NH**]$^{2+}$ vs. 108.3/[**B2-PdH**]$^{2+}$ kJ/mol) and the reductive elimination transition state (12.1/**TS7B** vs. 105.0/**TS7B'** kJ/mol). Comparison with the hydrogenolysis step without excess acid (Figure 6), the ligand-assisted protonation and reductive elimination is 19.1 kJ/mol more favored kinetically (12.1 vs. 31.2 kJ/mol); and this reveals that the excess of acid can accelerate the formation of (*Z*)-**3** by lowering the barrier.

Since the strong acid in solution can have dissociation equilibrium ($CF_3SO_3H \rightarrow CF_3SO_3^- + H^+$), we computed the effect of CF_3SO_3H in the formation of alkene either via only H-O in mono-dentate form (path **V**) or bidentate chelating form via both H-O and another O at sulfur center (path **VI**). As shown in Figure 7 (red lines), path **V** is more favored in energy than path **VI** by 25.9 kJ/mol (33.1 vs. 59.0 kJ/mol); and the more favored transition state (**TS9B**) is higher in energy that the 2-pyridyl ligand-assisted protonation and hydrogenation (**TS7B**) (33.1 vs. 12.1 kJ/mol). Using less acidic PTSA, the barrier is even higher (> 80 kJ/mol). All these results indicate the decisive role of acid strength in determining the observed chemoselectivity.

To compare the role of acid strength and loading in more detail, we recomputed transition state (**TSB2-CO**) and product (**B2-CO**) in the presence of a proton (**NH-TSB2-CO** and **NH-B2-CO**) as well as the following hydroformylation reaction (see *Supporting Information*). The transition states for hydrogenolysis and CO coordination under protonation, **NH-TS3B'** and **NH-TSB2-CO**, are given in Figure 3 (in pink). It is observed that protonation raises the energy of **TSB2-CO** and **B2-CO** by 14.1 and 31.5 kJ/mol. Taking **NH-TSB2-CO** as reference (23.0 kJ/mol), the barrier (12.1 kJ/mol) for the formation of alkene (*Z*)-**3** is lower than CO coordination by 10.9 kJ/mol. Besides, the energy barrier of hydrogenation (74.0 kJ/mol) is lower than hydroformylation (111.0 kJ/mol for **B3** as reference state) by 37.0 kJ/mol in the presence of triflic acid. This indicates that strong acid lowers the barrier of hydrogenation and raises the barrier of hydroformylation to a large extent, which ultimately results in a chemoselectivity switch. In addition, the regeneration of the active catalyst is lower in energy and does not affect the reaction rate and the chemoselectivity (Figure 7).

To understand the effect of the acid in more detail, several control experiments were also performed: When D_2 was used instead of H_2 in the presence of 1.0 equiv. of triflic acid, 42% protium was incorporated into the product of (*E*)-**3**, demonstrating the involvement of the acid in the protonation of the Pd-alkenyl complex (Scheme 3, a). In addition, the (*E*)-alkene is afforded without hydrogen gas in the presence of 100 mol% of Pd(0), 120 mol% of ligand and 200 mol% of triflic acid (Scheme 3b, entry 1). Notably, there was no reaction without acid or when using Pd(II) as catalyst precursor (Scheme 3b, entries 2 and 3). Besides, when using a large excess of CF_3SO_3H (4.0 equiv.) minor amounts (5%) of the fully hydrogenated product (1,2-diphenylethane) was observed (Scheme 3b, entry 4), which hints towards the possibility to protonate also the corresponding Pd alkyl complex.

Scheme 3. Pd-catalyzed semi-hydrogenation of diphenylacetylene: Mechanistic experiments.

(a) Deuterated labeling experiments

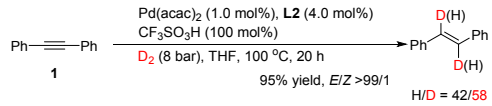

(b) Stoichiometric experiments

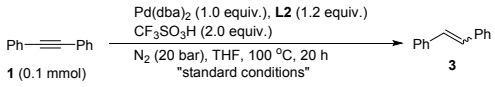

entry	variation from standard conditions	yield of **3** (*E*/*Z*)
1	none	95% (>99/1)
2	no acid	0%
3	$Pd(acac)_2$ was used instead of $Pd(dba)_2$	0%
4	4.0 equiv. CF_3SO_3H was used	95% (>99/1)

(c) Reactions using weak acid

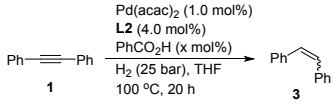

entry	x	conv. (%)	yield of **3** (*E*/*Z*)
1	16	58	55 (5/95)
2	32	97	94 (2/98)

To demonstrate that protonation of the intermediate Pd-alkenyl complex releases the *cis*-alkene (*Z*)-**3** first, the hydrogenation of the model substrate was performed in the presence of a weaker carboxylic acid (benzoic acid). Indeed, (*Z*)-**3** was detected in 94% yield with 98% stereoselectivity under these conditions(Scheme 3c, entry 2). At this point, it should be noted that this observation also provides the basis for the development of stereodivergent hydrogenations of alkynes depending on acidic co-catalyst.

Scheme 4. Isomerization from (*Z*)-3 to (*E*)-3: Control experiments

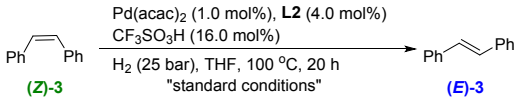

entry	variation from standard conditions	yield of (*E*)-3
1	none	>99%
2	no acid	6%
3	no ligand	0%
4	no [Pd]	<5%
5	no acid, no [Pd]	0%
6	no acid, no ligand	0%
7	no [Pd], no ligand	7%

[a]Reaction conditions: (*Z*)-**3** (0.3 mmol), $Pd(acac)_2$ (0.91 mg, 1.0 mol%), CF_3SO_3H (4.1μL, 16.0 mol%), **L2** (6.1 mg, 4.0 mol%) and H_2 (25 bar), 100 ˚C, 20 h, THF (1.0 mL). The yield of (*E*)-**3** was determined by GC analysis.

Scheme 5. Plausible catalytic cycle for hydroformylation and semi-hydrogenation

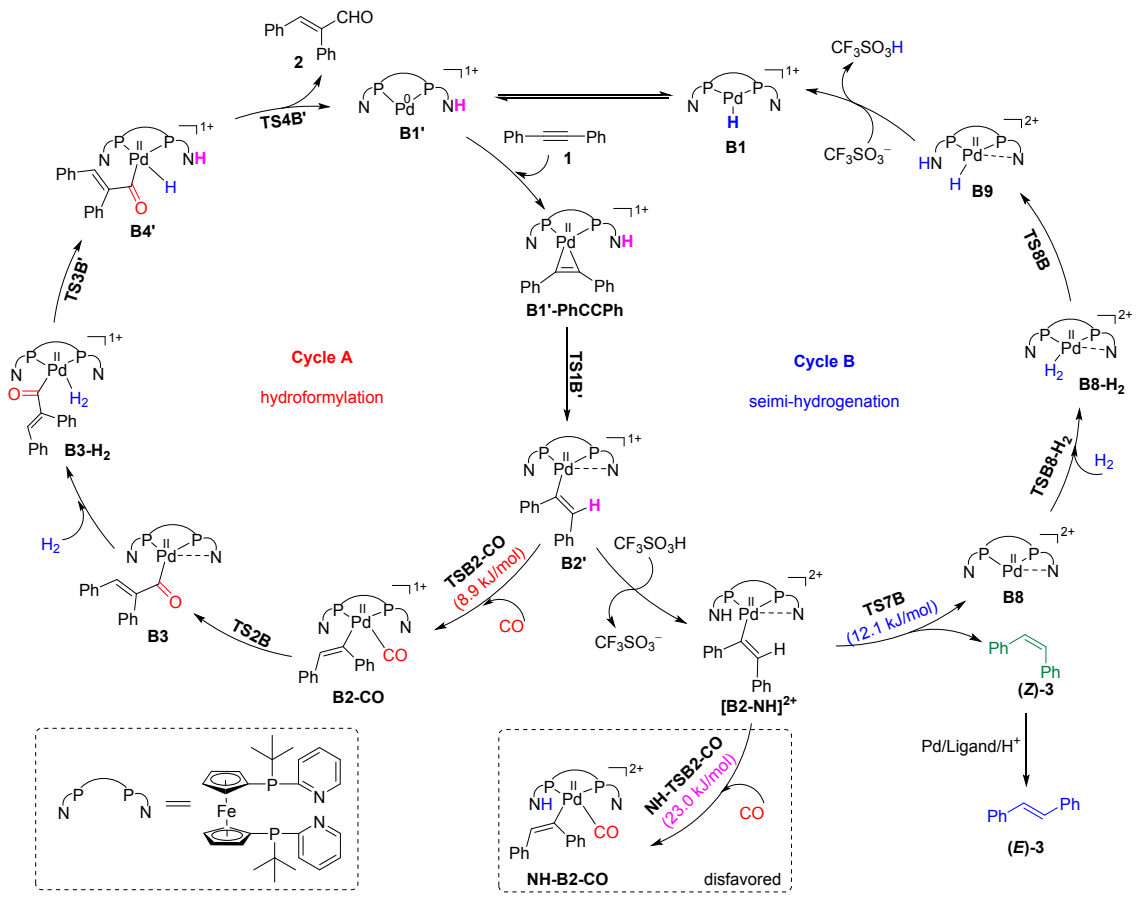

To further probe the isomerization process, (*Z*)-**3** was exposed to various catalytic reaction conditions. As shown in Scheme 4, the isomerization occurred smoothly under standard conditions to afford (*E*)-**3** in quantitative yield (Scheme 4, entry 1). Almost no conversion was observed without acid or palladium precursor or ligand, which indicated that all of them are crucial for this isomerization step. It is worth noting that during the isomerization of *Z*-alkene to *E*-alkene, there is no alkane generated via the protonation of alkyl-Pd intermediate. The probable reason is that the β-hydrogen elimination of alkyl-Pd complex is faster than protonation, which should be one of the main factors to achieve the alkene products selectively.

On the basis of all these experiments and DFT calculations we propose the following catalytic cycle for both hydroformylation and semi-hydrogenation of **1** in the presence of ligand **L2** (Scheme 5). This proposal is also supported by previous mechanistic work on alkoxycarbonylations using ligands **L1**-**L4**[18,19a] as well as related mechanistic studies by Cole-Hamilton,[19c] Drent[19b] and Sparkes[19d].

Initially, the stable Pd(II) precursor is *in situ* reduced to Pd(0) in the presence of excess amount of phosphine ligands,[25] followed by protonation to afford the active palladium hydride complex **B1**, which is probably in equilibrium with the *N*-protonated pyridinium complex **B1'**.[19a] Subsequently, alkyne coordination to palladium center occurs, leading to the formation of palladacyclopropene complex **B1'-PhCCPh**. Then, proton transfer takes place via the transition state **TS1B'** to afford the Pd-alkenyl complex **B2'**, which is the key intermediate for both hydroformylation and semi-hydrogenation. In the presence of weak acids or low concentration of stronger acids, the CO coordination and insertion process are kinetically favored, providing the acyl Pd-complex **B3**. Afterwards, *N*-assisted hydrogenolysis of **B3'** via transition state **TS3B'** affords the aldehyde **2** and regenerates the active *N*-protonated pyridinium species **B1'** to finish the cycle A. In the presence of sufficient concentration of strong acid, the direct protonation of the Pd-alkenyl complex **B2'** occurs to give the intermediate **[B2-NH]$^{2+}$**. After the transfer protonation via transition state **TS7B**, the olefin (*Z*)-**3** and Pd complex **B8** are afforded. *N*-Assisted hydrogenolysis of **B8** regenerates the acid and active Pd species **B1'** to conclude cycle B, and isomerization of (*Z*)-**3** in the presence of Pd/ligand/acid provides the final product (*E*)-**3**. It should be pointed out that after formation of **[B2-NH]$^{2+}$**, subsequent CO coordination to afford **NH-B2-CO** is disfavored compared with the proton transfer to give (*E*)-**3** and **B8** (23.0 kJ/mol *vs.* 12.1 kJ/mol). It is noted that in proposal a very important factor is the presence of neutral and mono cationic species in the hydroformylation cycle versus the dicationic complexes in the semi-hydrogenation cycle. Increasing the positive charge on the Pd complex, even if it is associated with a pendent protonated pyridine, should probably increase the positive charge on the Pd center and make the second pyridine coordination more likely that blocks CO coordination. That will slow hydroformylation and increase the protonation of the Pd-alkenyl intermediate to kick off alkene[26].

A general catalytic hydroformylation of alkynes: Following our original goal discussed in the introduction *vide supra*, we explored the general compatibility of this chemodivergent catalyst/co-catalyst system to a broader scope of alkynes. First, we studied the hydroformylation of various alkynes in the presence of PTSA as co-catalyst. As shown in Table 2, an array of symmetrical diaryl-substituted alkynes bearing neutral,

electron-deficient, and electron-rich substituents on the phenyl ring, underwent efficient hydroformylation to afford the corresponding α,β-unsaturated aldehydes (**6-12**, and **15**) in 60-92% yield with excellent *E* stereoselectivity. As an example, the thiofuran-substituted alkyne proved to be feasible in this reaction, providing product **13** in 62% yield. Pleasingly, a bulky substrate smoothly gave the corresponding product **14** in 82% yield with 95/5 stereoselectivity. Since unsymmetrical alkynes are more attractive from the viewpoint of organic synthesis, a series of such alkynes were investigated under standard conditions to afford the regioselective hydroformylation products in good yield and selectivity. More specifically, dialkyl-substituted internal alkyne led to the single isomer **16** in 58% yield and excellent stereoselectivity (>20/1); albeit with only moderate regioselectivity (70/30). Using unsymmetrical internal alkynes with aryl and alkyl substituents, hydroformylation mainly took place at the benzylic position, which can be attributed to the formation of the energetically favored vinyl palladium species, which is stabilized by aryl groups.

Table 2. Pd-catalyzed hydroformylation of various alkynes under syngas conditions [a]

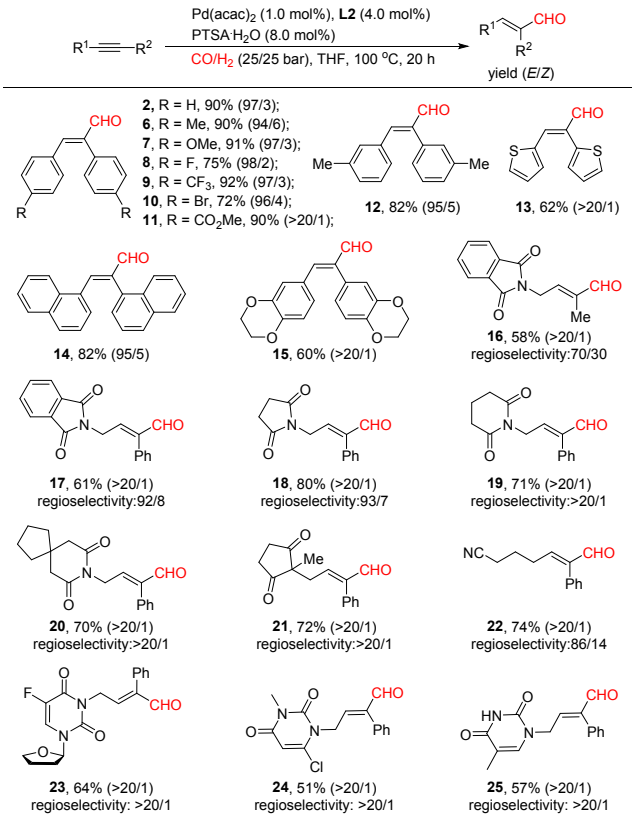

[a] Unless otherwise noted, all reactions were performed in THF (1.0 mL) at 100 °C for 20 h in the presence of alkynes (0.3 mmol), $Pd(acac)_2$ (0.91 mg, 1.0 mol%), PTSA·H_2O (4.8 mg, 8.0 mol%), **L2** (6.1 mg, 4.0 mol%) and CO/H_2 (25/25 bar). The *E*/*Z* selectivity were determined by GC and GC-MS analysis. The regioselectivity was determined by ^{1}H NMR analysis of crude products.

Thus, several aldehydes (**17-25**) were provided in 51-80% yield with 86/14->20/1 regioselectivity. Notably, this methodology showed excellent functional group tolerance, since bromide, ester, cyano, imide and ketone substituents were not touched. In addition, reactions of alkynes derivatized from uracil, one of the nucleobases of RNA, progressed well to give the corresponding aldehydes (**23-25**). However, using standard conditions, simple phenylacetylene gave only less than 5% of the corresponding aldehyde.

A general catalytic semi-hydrogenation of alkynes: Next, most of these alkynes were submitted to semi-hydrogenation under exactly the same conditions except using triflic acid instead of PTSA. As shown in Table 3, the corresponding alkenes were efficiently produced in good to high yield with excellent *E* stereoselectivity. In all cases, the corresponding aldehydes were only detected in trace amounts (<5%). With regard to synthetic applications, it is interesting that reducible functional groups such as ester, cyano, imide and even ketone survived in this hydrogenation process and the corresponding products (**31**, **34-41**) were obtained in good yield with excellent *E* stereoselectivity. Notably, alkyl-substituted alkynes may undergo further isomerization to provide a mixture of olefins; no such by-products were observed in presented cases because of the conjugation effect. Nevertheless, when using 4-octyne and 5-decyne, a mixture of alkenes was obtained (*Scheme S4*).

Finally, it should be pointed out that alkene **41** was generated from the corresponding nucleoside derivative by semi-hydrogenation of the alkyne and direct removal of the 2-furanyl group. This cascade sequence is explained by the acid-catalyzed hydrolysis of the N,O-acetal structure.

Table 3. Pd-catalyzed *E*-selective semi-hydrogenation of various alkynes under syngas conditions [a]

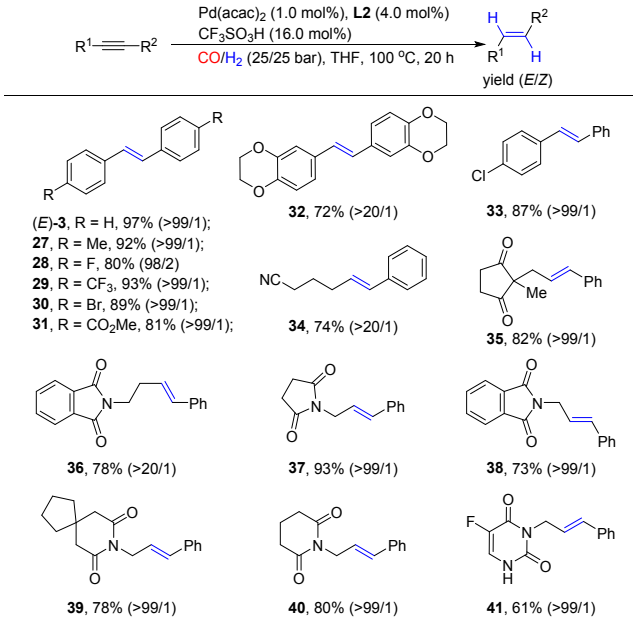

[a] Unless otherwise noted, all reactions were performed in THF (1.0 mL) at 100 °C for 20 h in the presence of alkynes (0.3 mmol), $Pd(acac)_2$ (0.91 mg, 1.0 mol%), CF_3SO_3H (4.1μL, 16.0 mol%), L2 (6.1 mg, 4.0 mol%) and CO/H_2 (25/25 bar). The *E*/*Z* selectivity were determined by GC, GC-MS and ^{1}H NMR analysis.

CONCLUSION

In summary, we describe the critical effect of acid strength and concentration for controlling the selectivity in palladium-catalyzed reactions of alkynes. This observation allowed for developing chemodivergent functionalizations of alkynes to afford a range of α,β-unsaturated aldehydes and alkenes in the presence of the same catalyst under similar conditions (temperature, solvent, pressure). Excellent selectivity control is achieved by employing an advanced Pd catalyst with **L2** as the

specified ligand. Mechanistic instigations and detailed DFT calculations provide rational explanation for this behavior. The insight of this tunable transformation comes from the specific role of the built-in 2-pyridyl substituent as base, which can lower the barrier of the hydrogenolysis step via a Frustrated Lewis Pair like process and accelerate the hydroformylation on one hand; and on the other hand, as a proton shuttle to suppress CO coordination to promote semi-hydrogenation under strong acid condition. This switchable selectivity using co-catalyst provides a new strategy in designing new catalysts for desired transformation and products.

AUTHOR INFORMATION

Corresponding Authors

Haijun.Jiao@catalysis.de

Matthias.Beller@catalysis.de

Author Contributions

‖ These authors contributed equally.

Notes

The authors declare no competing financial interest.

ASSOCIATED CONTENT

Supporting Information

Additional experimental results and procedures, characterization data of compounds as well as DFT calculation details. This material is available free of charge via the Internet at http://pubs.acs.org

ACKNOWLEDGMENT

This work is supported by BMBF (Bundesministerium für Bildung und Forschung), and the State of Mecklenburg-Vorpommern. We thank the analytical team of LIKAT for their kind support. J. Y. thanks the Chinese Scholarship Council (CSC) for financial support. This work is dedicated to the 70th anniversary of the Shanghai Institute of Organic Chemistry, Chinese Academy of Sciences.

REFERENCES

(1) For selected books and reviews, see: (a) Nakamura, A. Selectivity Control in Homogeneous Catalysis. In *Fundamental Research in Homogeneous Catalysis*; Tsutsui, M. Ed.; Springer: Boston, MA, 1979; pp 41-54; (b) Suib, S. L. Selectivity in Catalysis-An Overview, *ACS Symp. Ser.*, **1993**, *517*, 1-19; (c) Afagh, N. A.; Yudin, A. K., Chemoselectivity and the Curious Reactivity Preferences of Functional Groups. *Angew. Chem. Int. Ed.* **2010**, *49*, 262-310; (d) Hartwig, J. F., Regioselectivity of the Borylation of Alkanes and Arenes. *Chem. Soc. Rev.* **2011**, *40*, 1992-2002; (e) Neufeldt, S. R.; Sanford, M. S., Controlling Site Selectivity in Palladium-Catalyzed C–H Bond Functionalization. *Acc. Chem. Res.* **2012,** *45*, 936-946; (f) *Site-Selective Catalysis,* Topics in Current Chemistry; Kawabata, T., Ed.; Springer: Heidelberg, 2016; Vol. *372*, p 236; (g) Volkov, A.; Tinnis, F.; Slagbrand, T.; Trillo, P.; Adolfsson, H., Chemoselective Reduction of Carboxamides. *Chem. Soc. Rev.* **2016,** *45*, 6685-6697; (h) Huang, Z.; Dong, G., Site-Selectivity Control in Organic Reactions: A Quest To Differentiate Reactivity among the Same Kind of Functional Groups. *Acc. Chem. Res.* **2017,** *50*, 465-471; (i) Yang, B.; Qiu, Y.; Bäckvall, J.-E., Control of Selectivity in Palladium(II)-Catalyzed Oxidative Transformations of Allenes. *Acc. Chem. Res.* **2018**, 51, 1520-1531.

(2) Galloway, W. R. J. D.; Isidro-Llobet, A.; Spring, D. R., Diversity-oriented Ssynthesis as a Tool for the Discovery of Novel Biologically Active Small Molecules. *Nat. Commun.* **2010,** *1*, 80; (b) O' Connor, C. J.; Beckmann, H. S. G.; Spring, D. R., Diversity-Oriented Synthesis: Producing Chemical Tools for Dissecting Biology. *Chem. Soc. Rev.* **2012,** *41*, 4444-4456; (c) Guo, Z.; Yan, C.; Zhu, W.-H., High-Performance Quinoline-Malononitrile Core as a Building Block for the Diversity-Oriented Synthesis of AIEgens. *Angew. Chem. Int. Ed.* **2020,** *59*, 9812-9825; (d) Mortensen, K. T.; Osberger, T. J.; King, T. A.; Sore, H. F.; Spring, D. R., Strategies for the Diversity-Oriented Synthesis of Macrocycles. *Chem. Rev.* **2019,** *119*, 10288-10317; (e) Tejedor, D.; López-Tosco, S.; Méndez-Abt, G.; Cotos, L.; García-Tellado, F., Propargyl Vinyl Ethers and Tertiary Skipped Diynes: Two Pluripotent Molecular Platforms for Diversity-Oriented Synthesis. *Acc. Chem. Res.* **2016,** *49*, 703-713.

(3) For selected reviews and examples, see: (a) Beletskaya, I. P.; Nájera, C.; Yus, M., Stereodivergent Catalysis. *Chem. Rev.* **2018,** *118*, 5080-5200; (b) Nájera, C.; Beletskaya, I. P.; Yus, M., Metal-Catalyzed Regiodivergent Organic Reactions. *Chem. Soc. Rev.* **2019,** *48*, 4515-4618; (c) Peng, J.-B.; Wu, X.-F., Ligand- and Solvent-Controlled Regio- and Chemodivergent Carbonylative Reactions. *Angew. Chem. Int. Ed.* **2018,** *57*, 1152-1160; (d) Shen, C.; Wei, Z.; Jiao, H.; Wu, X.-F., Ligand- and Solvent-Tuned Chemoselective Carbonylation of Bromoaryl Triflates. *Chem. Eur. J.* **2017,** *23*, 13369-13378; (e) Xu, T.; Sha, F.; Alper, H., Highly Ligand-Controlled Regioselective Pd-Catalyzed Aminocarbonylation of Styrenes with Aminophenols. *J. Am. Chem. Soc.* **2016,** *138*, 6629-6635; (f) Wu, F.-P.; Peng, J.-B.; Meng, L.-S.; Qi, X.; Wu, X.-F., Palladium-Catalyzed Ligand-Controlled Selective Synthesis of Aldehydes and Acids from Aryl Halides and Formic Acid. *ChemCatChem* **2017,** *9*, 3121-3124; (g) Li, M.-B.; Inge, A. K.; Posevins, D.; Gustafson, K. P. J.; Qiu, Y.; Bäckvall, J.-E., Chemodivergent and Diastereoselective Synthesis of γ-Lactones and γ-Lactams: A Heterogeneous Palladium-Catalyzed Oxidative Tandem Process. *J. Am. Chem. Soc.* **2018,** *140*, 14604-14608; (h) Nguyen, V. D.; Nguyen, V. T.; Haug, G. C.; Dang, H. T.; Arman, H. D.; Ermler, W. C.; Larionov, O. V. Rapid and Chemodivergent Synthesis of *N*-Heterocyclic Sulfones and Sulfides: Mechanistic and Computational Details of the Persulfate-Initiated Catalysis. *ACS Catal.* **2019,** *9*, 4015-4024; (i) Qian, D.; Hu, X. Ligand-Controlled Regiodivergent Hydroalkylation of Pyrrolines. *Angew. Chem. Int. Ed.* **2019,** *58*, 18519-18523; (j) Singha, S.; Serrano, E.; Mondal, S.; Daniliuc, C. G.; Glorius, F., Diastereodivergent Synthesis of Enantioenriched α,β-Disubstituted γ-Butyrolactones via Cooperative *N*-Heterocyclic Carbene and Ir Catalysis. *Nat. Catal.* **2020,** *3*, 48-54; (k) Krautwald, S.; Sarlah, D.; Schafroth, M. A.; Carreira, E. M., Enantio- and Diastereodivergent Dual Catalysis: α-Allylation of Branched Aldehydes. *Science* **2013,** *340*, 1065-1068.

(4) (a) Hydroformylation: Fundamentals, Processes, and Application in Organic Synthesis; Börner, A., Franke, R., Eds.; Wiley-VCH: Weinheim, 2016. (b) Taddei, M.; Mann, A. *Hydroformylation for Organic Synthesis in Topics in Current Chemistry*; Springer: Berlin, 2013; Vol. *342*; (c) Franke, R.; Selent, D.; Börner, A. Applied Hydroformylation. *Chem. Rev.* **2012**, *112*, 5675−5732. (d) Wiese, K.-D.; Obst, D. Hydroformylation. In *Catalytic Carbonylation Reactions*; Beller, M., Ed.; Springer-Verlag: Berlin, 2010; pp 1-33; (e) Kelkar, A. A., Chapter 14-Carbonylations and Hydroformylations for Fine Chemicals. In *Industrial Catalytic Processes for Fine and Specialty Chemicals*, Joshi, S. S.; Ranade, V. V., Eds. Elsevier: Amsterdam, 2016; pp 663-692; (f) Herwig, J.; Fischer, R. Aqueous Biphasic Hydroformylation. In: *Rhodium Catalyzed Hydroformylation*, Van Leeuwen P. W. N. M., Claver C. Eds.; Springer: Dordrecht, 2000; vol *22*, pp 189-202.

(5) For selected reviews, see: (a) Li, S.; Li, Z.; You, C.; Lv, H.; Zhang, X. Recent Advances in Asymmetric Hydroformylation. *Chin. J. Org. Chem.* **2019,** *39*, 1568-1582; (b) Pospech, J.; Fleischer, I.; Franke, R.; Buchholz, S.; Beller, M., Alternative Metals for Homogeneous Catalyzed Hydroformylation Reactions. *Angew. Chem. Int. Ed.* **2013,** *52*, 2852-2872; (c) Breit, B. Recent Advances in Alkene Hydroformylation. In *Metal Catalyzed Reductive C–C Bond Formation*; Krische M. J. Ed.; Springer: Berlin, Heidelberg, 2007; pp 139-172; (d) Jia, X.; Wang, Z.; Xia, C.; Ding, K., Recent Advances in Rh-Catalyzed Asymmetric Hydroformylation of Olefins. *Chin. J. Org. Chem.*, **2013**, *33*, 1369-1381; (e) Bohnen, H.-W.; Cornils, B., Hydroformylation of Alkenes: An Industrial View of the Status and

Importance. In *Advances in Catalysis*; Academic Press, 2002; Vol. *47*, pp 1-64.; (f) Agbossou, F.; Carpentier, J. -F.; Mortreux, A., Asymmetric Hydroformylation. *Chem. Rev.* **1995,** *95*, 2485-2506.

(6) For selected recent examples, see: (a) Hood, D. M.; Johnson, R. A.; Carpenter, A. E.; Younker, J. M.; Vinyard, D. J.; Stanley, G. G., Highly Active Cationic Cobalt(II) Hydroformylation Catalysts. *Science* **2020,** *367*, 542-548; (b) You, C.; Li, S.; Li, X.; Lan, J.; Yang, Y.; Chung, L. W.; Lv, H.; Zhang, X., Design and Application of Hybrid Phosphorus Ligands for Enantioselective Rh-Catalyzed Anti-Markovnikov Hydroformylation of Unfunctionalized 1,1-Disubstituted Alkenes. *J. Am. Chem. Soc.* **2018,** *140*, 4977-4981; (c) Phanopoulos, A.; Nozaki, K., Branched-Selective Hydroformylation of Nonactivated Olefins Using an *N*-Triphos/Rh Catalyst. *ACS Catal.* **2018,** *8*, 5799-5809; (d) Ren, W.; Chang, W.; Dai, J.; Shi, Y.; Li, J.; Shi, Y., An Effective Pd-Catalyzed Regioselective Hydroformylation of Olefins with Formic Acid. *J. Am. Chem. Soc.* **2016,** *138*, 14864-14867; (e) You, C.; Li, X.; Yang, Y.; Yang, Y.-S.; Tan, X.; Li, S.; Wei, B.; Lv, H.; Chung, L.-W.; Zhang, X., Silicon-Oriented Regio- and Enantioselective Rhodium-Catalyzed Hydroformylation. *Nat. Commun.* **2018,** *9*, 2045; (f) Ren, X.; Zheng, Z.; Zhang, L.; Wang, Z.; Xia, C.; Ding, K., Rhodium-Complex-Catalyzed Hydroformylation of Olefins with CO_2 and Hydrosilane. *Angew. Chem. Int. Ed.* **2017,** *56*, 310-313; (g) Dingwall, P.; Fuentes, J. A.; Crawford, L.; Slawin, A. M. Z.; Bühl, M.; Clarke, M. L., Understanding a Hydroformylation Catalyst that Produces Branched Aldehydes from Alkyl Alkenes. *J. Am. Chem. Soc.* **2017,** *139*, 15921-15932.

(7) (a) Green-field, H.; Wotiz, J. H.; Wender, I. Reactions of Acetylenic Compounds under Hydroformylation Conditions. *J. Org. Chem.* **1957**, *22*, 542-546; (b) Johnson, J. R.; Cuny, G. D.; Buchwald, S. L. Rhodium-Catalyzed Hydroformylation of Internal Alkynes to α,β-Unsaturated Aldehydes. *Angew. Chem., Int. Ed. Engl.* **1995**, *34*, 1760-1761; (c) Van den Hoven, B. G.; Alper, H., Regioselective Hydroformylation of Enynes Catalyzed by a Zwitterionic Rhodium Complex and Triphenyl Phosphite. *J. Org. Chem.* **1999,** *64*, 3964-3968; (d) Van den Hoven, B. G.; Alper, H., The First Regioselective Hydroformylation of Acetylenic Thiophenes Catalyzed by a Zwitterionic Rhodium Complex and Triphenyl Phosphite. *J. Org. Chem.* **1999,** *64*, 9640-9645; (e) Agabekov, V.; Seiche, W.; Breit, B., Rhodium-catalyzed Hydroformylation of Alkynes Employing a Self-Assembling Ligand System. *Chem. Sci.* **2013,** *4*, 2418-2422; (f) Zhang, Z.; Wang, Q.; Chen, C.; Han, Z.; Dong, X. Q.; Zhang, X., Selective Rhodium-Catalyzed Hydroformylation of Alkynes to α,β-Unsaturated Aldehydes with a Tetraphosphoramidite Ligand. *Org. Lett.* **2016,** *18*, 3290-3293; (g) Tan, G.; Wu, Y.; Shi, Y.; You, J., Syngas-Free Highly Regioselective Rhodium-Catalyzed Transfer Hydroformylation of Alkynes to α, β-Unsaturated Aldehydes. *Angew. Chem. Int. Ed.* **2019,** *58*, 7440-7444; (h) Wagner, P.; Donnard, M.; Girard, N., Ligand-Controlled Regiodivergent Hydroformylation of Ynamides: A Stereospecific and Regioselective Access to 2- and 3-Aminoacroleins. *Org. Lett.* **2019,** *21*, 8861-8866.

(8) (a) Ishii, Y.; Miyashita, K.; Kamita, K.; Hidai, M., Selective Hydroformylation of Internal Acetylenes by $PdCl_2(PCy_3)_2$: Remarkable Synergistic Effect of Cobalt. *J. Am. Chem. Soc.* **1997,** *119*, 6448-6449; (b) Liu, Y.; Cai, L.; Xu, S.; Pu, W.; Tao, X., Palladium-Catalyzed Hydroformylation of Terminal Arylacetylenes with Glyoxylic Acid. *Chem. Commun.* **2018,** *54*, 2166-2168; (c) Fang, X.; Zhang, M.; Jackstell, R.; Beller, M., Selective Palladium-Catalyzed Hydroformylation of Alkynes to α, β-Unsaturated Aldehydes. *Angew. Chem. Int. Ed.* **2013,** *52*, 4645-4649.

(9) (a) Swamy, K. C. K.; Reddy, A. S.; Sandeep, K.; Kalyani, A., Advances in Chemoselective and/or Stereoselective Semihydrogenation of Alkynes. *Tetrahedron Lett.* **2018,** *59*, 419-429; (b) de Vries, J. G., Elsevier, C. J., Eds. *The Handbook of Homogeneous Hydrogenation*; Wiley-VCH: Weinheim, **2007**; (c) Oger, C.; Balas, L.; Durand, T.; Galano, J.-M., Are Alkyne Reductions Chemo-, Regio-, and Stereoselective Enough To Provide Pure (*Z*)-Olefins in Polyfunctionalized Bioactive Molecules? *Chem. Rev.* **2013,** *113*, 1313-1350.

(10) Lindlar, H.; Dubuis, R. Palladium Catalyst for Partial Reduction of Acetylenes. *Org. Synth.* **1966**, *46*, 89.

(11) (a) Pelagatti, P.; Venturini, A.; Leporati, A.; Carcelli, M.; Costa, M.; Bacchi, A.; Pelizzi, G.; Pelizzi, C., Chemoselective Homogeneous Hydrogenation of Phenylacetylene Using Thiosemicarbazone and Thiobenzoylhydrazone Palladium(II) Complexes as Catalysts. *J. Chem. Soc., Dalton Trans.* **1998,** 2715-2722; (b) Tani, K.; Iseki, A.; Yamagata, T., Efficient Transfer Hydrogenation of Alkynes and Alkenes with Methanol Catalysed by Hydrido(methoxo)iridium(III) Complexes. *Chem. Commun.* **1999,** 1821-1822; (c) van Laren, M. W.; Elsevier, C. J., Selective Homogeneous Palladium (0)-Catalyzed Hydrogenation of Alkynes to (*Z*)-Alkenes. *Angew. Chem. Int. Ed.* **1999,** *38*, 3715-3717; (d) Trost, B. M.; Ball, Z. T.; Jöge, T., A Chemoselective Reduction of Alkynes to (*E*)-Alkenes. *J. Am. Chem. Soc.* **2002,** *124*, 7922-7923; (e) Shirakawa, E.; Otsuka, H.; Hayashi, T., Reduction of Alkynes into 1,2-Dideuterioalkenes with Hexamethyldisilane and Deuterium Oxide in the Presence of a Palladium Catalyst. *Chem. Commun.* **2005**, 5885-5886; (f) Shen, R.; Chen, T.; Zhao, Y.; Qiu, R.; Zhou, Y.; Yin, S.; Wang, X.; Goto, M.; Han, L. B., Facile Regio- and Stereoselective Hydrometalation of Alkynes with a Combination of Carboxylic Acids and Group 10 Transition Metal Complexes: Selective Hydrogenation of Alkynes with Formic Acid. *J. Am. Chem. Soc.* **2011,** *133*, 17037-17044; (g) Yan, M.; Jin, T.; Ishikawa, Y.; Minato, T.; Fujita, T.; Chen, L. Y.; Bao, M.; Asao, N.; Chen, M. W.; Yamamoto, Y., Nanoporous Gold Catalyst for Highly Selective Semihydrogenation of Alkynes: Remarkable Effect of Amine Additives. *J. Am. Chem. Soc.* **2012,** *134*, 17536-17542; (h) Radkowski, K.; Sundararaju, B.; Fürstner, A., A Functional-Group-Tolerant Catalytic trans Hydrogenation of Alkynes. *Angew. Chem. Int. Ed.* **2013,** *52*, 355-360; (i) Drost, R. M.; Bouwens, T.; van Leest, N. P.; de Bruin, B.; Elsevier, C. J., Convenient Transfer Semihydrogenation Methodology for Alkynes Using a Pd^{II}-NHC Precatalyst. *ACS Catal.* **2014,** *4*, 1349-1357; (j) Karunananda, M. K.; Mankad, N. P., *E*-Selective Semi-Hydrogenation of Alkynes by Heterobimetallic Catalysis. *J. Am. Chem. Soc.* **2015,** *137*, 14598-601; (k) Mitsudome, T.; Urayama, T.; Yamazaki, K.; Maehara, Y.; Yamasaki, J.; Gohara, K.; Maeno, Z.; Mizugaki, T.; Jitsukawa, K.; Kaneda, K., Design of Core-Pd/Shell-Ag Nanocomposite Catalyst for Selective Semihydrogenation of Alkynes. *ACS Catal.* **2015,** *6*, 666-670; (l) Furukawa, S.; Komatsu, T., Selective Hydrogenation of Functionalized Alkynes to (*E*)-Alkenes, Using Ordered Alloys as Catalysts. *ACS Catal.* **2016,** *6*, 2121-2125; (m) Neumann, K. T.; Klimczyk, S.; Burhardt, M. N.; Bang-Andersen, B.; Skrydstrup, T.; Lindhardt, A. T., Direct *trans*-Selective Ruthenium-Catalyzed Reduction of Alkynes in Two-Chamber Reactors and Continuous Flow. *ACS Catal.* **2016,** *6*, 4710-4714; (n) Lu, Y.; Feng, X.; Takale, B. S.; Yamamoto, Y.; Zhang, W.; Bao, M., Highly Selective Semihydrogenation of Alkynes to Alkenes by Using an Unsupported Nanoporous Palladium Catalyst: No Leaching of Palladium into the Reaction Mixture. *ACS Catal.* **2017,** *7*, 8296-8303; (o) Siva Reddy, A.; Kumara Swamy, K. C., Ethanol as a Hydrogenating Agent: Palladium-Catalyzed Stereoselective Hydrogenation of Ynamides To Give Enamides. *Angew. Chem. Int. Ed.* **2017,** *56*, 6984-6988; (p) Guthertz, A.; Leutzsch, M.; Wolf, L. M.; Gupta, P.; Rummelt, S. M.; Goddard, R.; Fares, C.; Thiel, W.; Furstner, A., Half-Sandwich Ruthenium Carbene Complexes Link *trans*-Hydrogenation and *gem*-Hydrogenation of Internal Alkynes. *J. Am. Chem. Soc.* **2018,** *140*, 3156-3169; (q) Song, L.; Feng, Q.; Wang, Y.; Ding, S.; Wu, Y.-D.; Zhang, X.; Chung, L. W.; Sun, J., Ru-Catalyzed Migratory Geminal Semihydrogenation of Internal Alkynes to Terminal Olefins. *J. Am. Chem. Soc.* **2019,** *141*, 17441-17451; (r) Zhao, C.-Q.; Chen, Y.-G.; Qiu, H.; Wei, L.; Fang, P.; Mei, T.-S., Water as a Hydrogenating Agent: Stereodivergent Pd-Catalyzed Semihydrogenation of Alkynes. *Org. Lett.* **2019,** *21*, 1412-1416; (s) Wang, Y.; Huang, Z.; Huang, Z., Catalyst as Colour Indicator for Endpoint Detection to Enable Selective Alkyne *trans*-Hydrogenation with Ethanol. *Nature Catalysis* **2019,** *2*, 529-536.

(12) (a) Enthaler, S.; Haberberger, M.; Irran, E., Highly Selective Iron-Catalyzed Synthesis of Alkenes by the Reduction of Alkynes. *Chem. Asian. J.* **2011,** *6*, 1613-1623; (b) Srimani, D.; Diskin-Posner, Y.; Ben-David, Y.; Milstein, D., Iron Pincer Complex Catalyzed, Environmentally Benign, *E*-Selective Semi-Hydrogenation of Alkynes. *Angew. Chem. Int. Ed.* **2013,** *52* (52), 14131-14134; (c) Cao, H.; Chen, T.; Zhou, Y.; Han, D.; Yin, S.-F.; Han, L.-B., Copper-Catalyzed

Selective Semihydrogenation of Terminal Alkynes with Hypophosphorous Acid. *Adv. Synth. Catal.* **2014,** *356*, 765-769; (d) Richmond, E.; Moran, J., Ligand Control of *E*/*Z* Selectivity in Nickel-Catalyzed Transfer Hydrogenative Alkyne Semireduction. *J. Org. Chem.* **2015,** *80*, 6922-6929; (e) Fu, S.; Chen, N. Y.; Liu, X.; Shao, Z.; Luo, S. P.; Liu, Q., Ligand-Controlled Cobalt-Catalyzed Transfer Hydrogenation of Alkynes: Stereodivergent Synthesis of *Z*- and *E*-Alkenes. *J. Am. Chem. Soc.* **2016,** *138*, 8588-8594; (f) Raya, B.; Biswas, S.; RajanBabu, T. V., Selective Cobalt-Catalyzed Reduction of Terminal Alkenes and Alkynes Using $(EtO)_2Si(Me)H$ as a Stoichiometric Reductant. *ACS Catal* **2016,** *6*, 6318-6323; (g) Chen, C.; Huang, Y.; Zhang, Z.; Dong, X. Q.; Zhang, X., Cobalt-Catalyzed (*Z*)-Selective Semihydrogenation of Alkynes with Molecular Hydrogen. *Chem. Commun.* **2017,** *53*, 4612-4615; (h) Chen, F.; Kreyenschulte, C.; Radnik, J.; Lund, H.; Surkus, A.-E.; Junge, K.; Beller, M., Selective Semihydrogenation of Alkynes with *N*-Graphitic-Modified Cobalt Nanoparticles Supported on Silica. *ACS Catal.* **2017,** *7*, 1526-1532; (i) Brzozowska, A.; Azofra, L. M.; Zubar, V.; Atodiresei, I.; Cavallo, L.; Rueping, M.; El-Sepelgy, O., Highly Chemo- and Stereoselective Transfer Semihydrogenation of Alkynes Catalyzed by a Stable, Well-Defined Manganese(II) Complex. *ACS Catal.* **2018,** *8*, 4103-4109; (j) Gorgas, N.; Brünig, J.; Stöger, B.; Vanicek, S.; Tilset, M.; Veiros, L. F.; Kirchner, K., Efficient *Z*-Selective Semihydrogenation of Internal Alkynes Catalyzed by Cationic Iron(II) Hydride Complexes. *J. Am. Chem. Soc.* **2019,** *141*, 17452-17458; (k) Li, K.; Khan, R.; Zhang, X.; Gao, Y.; Zhou, Y.; Tan, H.; Chen, J.; Fan, B., Cobalt Catalyzed Stereodivergent Semi-Hydrogenation of Alkynes Using H_2O as the Hydrogen Source. *Chem. Commun.* **2019,** 5663-5666.

(13) (a) Takahashi, K.; Yamashita, M.; Ichihara, T.; Nakano, K.; Nozaki, K., High-Yielding Tandem Hydroformylation/Hydrogenation of a Terminal Olefin to Produce a Linear Alcohol Using a Rh/Ru Dual Catalyst System. *Angew. Chem. Int. Ed.* **2010,** *49*, 4488-4490; (b) Takahashi, K.; Yamashita, M.; Tanaka, Y.; Nozaki, K., Ruthenium/C_5Me_5/Bisphosphine- or Bisphosphite-Based Catalysts for Normal-Selective Hydroformylation. *Angew. Chem. Int. Ed.* **2012,** *51*, 4383-4387; (c) Takahashi, K.; Yamashita, M.; Nozaki, K., Tandem Hydroformylation/Hydrogenation of Alkenes to Normal Alcohols Using Rh/Ru Dual Catalyst or Ru Single Component Catalyst. *J. Am. Chem. Soc.* **2012,** *134*, 18746-18757; (d) Wu, L.; Fleischer, I.; Jackstell, R.; Beller, M., Efficient and Regioselective Ruthenium-catalyzed Hydro-aminomethylation of Olefins. *J. Am. Chem. Soc.* **2013,** *135*, 3989-3996; (e) Wu, L.; Fleischer, I.; Jackstell, R.; Profir, I.; Franke, R.; Beller, M., Ruthenium-Catalyzed Hydroformylation/Reduction of Olefins to Alcohols: Extending the Scope to Internal Alkenes *J. Am. Chem. Soc.* **2013,** *135*, 14306-14312; (f) Fang, W.; Breit, B., Tandem Regioselective Hydroformylation-Hydrogenation of Internal Alkynes Using a Supramolecular Catalyst. *Angew. Chem. Int. Ed.* **2018,** *57*, 14817-14821.

(14) Takahashi, K.; Nozaki, K., Ruthenium Catalyzed Hydrogenation of Aldehyde with Synthesis Gas. *Org. Lett.* **2014,** *16*, 5846-5849.

(15) Gianetti, T. L.; Tomson, N. C.; Arnold, J.; Bergman, R. G., Z-Selective, Catalytic Internal Alkyne Semihydrogenation under H_2/CO Mixtures by a Niobium(III) Imido Complex. *J. Am. Chem. Soc.* **2011,** *133*, 14904-14907.

(16) Jagtap, S. A.; Sasaki, T.; Bhanage, B. M., Silica Supported Palladium Phosphine as a Robust and Recyclable Catalyst for Semi-Hydrogenation of Alkynes Using Syngas. *J. Mol. Catal. A: Chem.* **2016,** *414*, 78-86.

(17) Jagtap, S. A.; Bhanage, B. M., Ligand Assisted Rhodium Catalyzed Selective Semi-Hydrogenation of Alkynes Using Syngas and Molecular Hydrogen. *ChemistrySelect* **2018,** *3*, 713-718.

(18) (a) Dong, K.; Fang, X.; Gülak, S.; Franke, R.; Spannenberg, A.; Neumann, H.; Jackstell, R.; Beller, M. Highly Active and Efficient Catalysts for Alkoxycarbonylation of Alkenes. *Nat. Commun.* **2017**, *8*, 14117; (b) Dong, K.; Sang, R.; Fang, X.; Franke, R.; Spannenberg, A.; Neumann, H.; Jackstell, R.; Beller, M. Efficient Palladium-Catalyzed Alkoxycarbonylation of Bulk Industrial Olefins Using Ferrocenyl Phosphine Ligands. *Angew. Chem. Int. Ed.* **2017**, *56*, 5267-5271; (c) Liu, J.; Dong, K.; Franke, R.; Neumann, H.; Jackstell, R.; Beller, M. Selective Palladium-Catalyzed Carbonylation of Alkynes: An Atom-Economic Synthesis of 1,4-Dicarboxylic Acid Diesters. *J. Am. Chem. Soc.* **2018**, *140*, 10282-10288; (d) Yang, J.; Liu, J.; Neumann, H.; Franke, R.; Jackstell, R.; Beller, M. Direct Synthesis of Adipic Acid Esters via Palladium-Catalyzed Carbonylation of 1,3-Dienes. *Science*, **2019**, *366*, 1514-1517; (e) Liu, J.; Yang, J.; Schneider, C.; Frank, R.; Jackstell, R.; Beller, M. Tailored Palladium Catalysts for Selective Synthesis of Conjugated Enynes by Monocarbonylation of 1,3-Diynes. *Angew. Chem. Int. Ed.* **2020**, *59*, 9032-9040.

(19) (a) Dong, K.; Sang, R.; Wei, Z.; Liu, J.; Dühren, R.; Spannenberg, A.; Jiao, H.; Neumann, H.; Jackstell, R.; Franke, R.; Beller, M. Cooperative Catalytic Methoxycarbonylation of Alkenes: Uncovering the Role of Palladium Complexes with Hemilabile Ligand. *Chem. Sci.* **2018**, *9*, 2510-2516; (b) Crawford, L.; Cole-Hamilton, D. J.; Drent, E.; Bühl, M. Mechanism of Alkyne Alkoxycarbonylation at a Pd Catalyst with *P*,*N* Hemilabile Ligands: A Density Functional Study. *Chem.-Eur. J.*, **2014**, *20*, 13923-13926; (c) Crawford, L.; Cole-Hamilton, D. J.; Bühl, M. Uncovering the Mechanism of Homogeneous Methyl Methacrylate Formation with *P*,*N* Chelating Ligands and Palladium: Favored Reaction Channels and Selectivities. *Organometallics*, **2015**, *34*, 438-449; (d) Shuttleworth, A.; Miles-Hobbs, A. M.; Pringle, P. G.; Sparkes, H. A. 2-Pyridyl Substituents Enhance the Activity of Palladium–Phospha-Adamantane Catalysts for the Methoxycarbonylation of Phenylacetylene. *Dalton Trans.* **2017**, *46*, 125-137.

(20) (a) Zhao, Y.; Truhlar, D. G., A New Local Density Functional for Main-Group Thermochemistry, Transition Metal Bonding, Thermochemical Kinetics, and Noncovalent Interactions. *J. Chem. Phys.* **2006**, *125*, 194101; (b) Zhao, Y.; Truhlar, D. G., The M06 Suite of Density Functionals for Main Group Thermochemistry, Thermochemical Kinetics, Noncovalent Interactions, Excited States, and Transition Elements: Two New Functionals and Systematic Testing of Four M06-Class Functionals and 12 Other Functionals. *Theor. Chem. Acc.* **2008**, *120*, 215-241; (c) Andrae, D.; Häußermann, U.; Dolg, M.; Stoll, H.; Preuß, H., Energy-Adjustedab Initio Pseudopotentials for the Second and Third Row Transition Elements. *Theor. Chim. Acta* **1990,** *77*, 123-141.

(21) (a) Becke, A. D., Density-Functional Thermochemistry. III. The Role of Exact Exchange. *J. Chem. Phys.* **1993,** *98*, 5648-5652; (b) Schäfer, A.; Huber, C.; Ahlrichs, R., Fully Optimized Contracted Gaussian Basis Sets of Triple Zeta Valence Quality for Atoms Li to Kr. *J. Chem. Phys.* **1994,** *100*, 5829-5835.

(22) Liu, J.; Wei, Z.; Jiao, H.; Jackstell, R.; Beller, M., Toward Green Acylation of (Hetero)Arenes: Palladium-Catalyzed Carbonylation of Olefins to Ketones. *ACS Cent Sci* **2018,** *4*, 30-38.

(23) (a) Welch, G. C.; San Juan, R. R.; Masuda, J. D.; Stephan, D. W. Reversible, Metal-Free Hydrogen Activation. *Science* **2006,** *314*, 1124-1126; (b) Welch, G. C.; Stephan, D. W., Facile Heterolytic Cleavage of Dihydrogen by Phosphines and Boranes. *J. Am. Chem. Soc.* **2007,** *129*, 1880-1881; (c) Hamza, A.; Stirling, A.; András Rokob, T.; Pápai, I., Mechanism of Hydrogen Activation by Frustrated Lewis Pairs: A Molecular Orbital Approach. *Int. J. Quantum. Chem.* **2009,** *109*, 2416-2425; (d) Liu, L.; Lukose, B.; Ensing, B. Hydrogen Activation by Frustrated Lewis Pairs Revisited by Metadynamics Simulations. *J. Phys. Chem. C* **2017,** *121*, 2046-2051; (e) Pu, M.; Privalov, T. How Frustrated Lewis Acid/Base Systems Pass through Transition-State Regions: H_2 Cleavage by $[^tBu_3P/B(C_6F_5)_3]$. *ChemPhysChem* **2014,** *15*, 2936-2944; (f) Welch, G. C.; Cabrera, L.; Chase, P. A.; Hollink, E.; Masuda, J. D.; Wei, P.; Stephan, D. W. Tuning Lewis Acidity Using the Reactivity of "Frustrated Lewis Pairs": Facile Formation of Phosphine-Boranes and Cationic Phosphonium-boranes. *Dalton Trans.* **2007**, 3407-3414.

(24) For the Comparable *PKa* Value of Four Acids, See the Following Website: http://www.periodensystem-online.de/index.php?sel=wertdesc&prop=pKs-Werte&show=list&id=acid

(25) (a) Amatore, C.; Jutand, A.; M'Barki, M. A. Evidence of the Formation of Zerovalent Palladium from $Pd(OAc)_2$ and Triphenylphosphine. *Organometallics* **1992**, *11*, 3009-3013; (b) Amatore, C.; Carre, E.; Jutand, A.; M'Barki, M. A. Rates and Mechanism of the Formation of Zerovalent Palladium Complexes from Mixtures of $Pd(OAc)_2$ and Tertiary Phosphines and Their Reactivity in Oxidative Additions. *Organometallics* **1995**, *14*, 1818-1826.

(26) Liu, J., Jacob, C., Sheridan, K. J., Al-Mosule, F., Heaton, B. T., Iggo, J. A., Matthews, M., Pelletier, J., Whyman, R., Bickley, J. F., Steiner, A. The Synthesis of, and Characterization of the Dynamic Processes Occurring in Pd(II) Chelate Complexes of 2-Pyridyldiphenylphosphine. *Dalton Trans.* **2010**, *39*, 7921-7935.

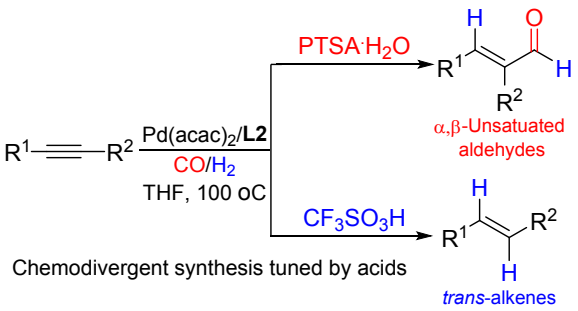

Chemodivergent synthesis tuned by acids